Upper and Lower Bounds on the Drag Coefficient of a Sphere in an Ellis Model Fluid

SCOTT W. HOPKE and JOHN C. SLATTERY

Northwestern University, Evanston, Illinois

Hill's extremum principles are not directly applicable to an Ellis model fluid. A method of adapting Hill's principles to the Ellis model was developed and used to calculate upper and lower bounds on the drag coefficient for a sphere moving slowly through such a fluid. Available experimental data were compared with the average of the upper and lower bounds. Agreement was poor with Slattery's data and good with Turian's data. Some reasons to suspect Slattery's data have been pointed out.

The equation of continuity and the stress equation of motion are not sufficient to describe the motion of a particular material under a given set of boundary conditions. As a minimum of additional information, we require a description of stress in the material as a function of deformation; this is usually referred to as a *constitutive equation* for stress. The subject of constitutive equations has been briefly reviewed previously (*1, 2*). It is sufficient to say that one of the simplest constitutive equations proposed for incompressible fluids is the incompressible Reiner-Rivlin model (3 to *6*), a special case of which is the generalized Newtonian fluid:

$$\mathbf{T}_E \equiv \mathbf{T} + p\,\mathbf{I} = 2\eta\,\mathbf{D} \tag{1}$$

Here

$$\mathbf{D} \equiv \frac{1}{2}\left[\nabla\mathbf{v} + (\nabla\mathbf{v})^T\right] \tag{2}$$

and

$$\eta = \eta(\gamma^2), \quad \gamma^2 \equiv tr(\mathbf{D}\cdot\mathbf{D}) \equiv D_{ij}D^{ji} \tag{3}$$

Two special cases of Equation (1) are the incompressible Newtonian fluid

$$\eta = \text{constant} \tag{4}$$

and the power model fluid

$$\eta = m\,[\sqrt{2}\gamma]^{n-1} \tag{5}$$

The power model fluid cannot fully represent the behavior of any real material presently known, since it does not predict nonzero limiting viscosities at very low and very high rates of deformation. On the other hand, over a limited range of stress it often gives a satisfactory approximation for the stress vs. rate-of-deformation curve from a viscometric study.

Another form of the incompressible generalized Newtonian fluid is

$$\mathbf{D} = \frac{1}{2}\Phi\,\mathbf{T}_E \tag{6}$$

where

$$\Phi = \Phi(\sigma^2), \quad \sigma^2 \equiv tr(\mathbf{T}_E\cdot\mathbf{T}_E) \tag{7}$$

A special case of Equation (6) is the three-parameter Ellis model (*7*):

$$\Phi = \frac{1}{\eta_0}\left\{1 + \left[\frac{\sigma}{\sqrt{2}\,\tau_{1/2}}\right]^{\alpha-1}\right\} \tag{8}$$

Illustrations of the use of Equation (8) to describe non-Newtonian viscosity data have been given recently by Sadowski (*8*); Ashare, Bird, and Lescarboura (*9*); Sutterby (*10*); and Turian (*11*). The Ellis model correctly predicts a nonzero viscosity in the limit as σ approaches zero but incorrectly predicts a zero viscosity in the limit as σ becomes unbounded. The Ellis model fluid includes the power model fluid as a special case when $\frac{1}{\eta_0} \to 0$ while $\frac{1}{\eta_0[\tau_{1/2}]^{\alpha-1}}$ remains finite.

Attempts to analyze flow past a sphere of viscoelastic fluids have been summarized elsewhere (*1, 12*). Three major approximations for the drag force on a sphere moving slowly through a power model fluid have been presented.

1. Tomita (*13*) [for corrections and refinements see (*12, 14*)] calculated an upper bound using a velocity variational principle which is a special case of a more general variational principle proposed by Pawlowski (*15*). His trial velocity distribution involved no undetermined parameters.
2. Slattery (*16*) used Pawlowski's variational principle to obtain an upper bound which was lower than that of Tomita for $n > 0.76$.
3. Wasserman and Slattery (*1*) obtained a much lower upper bound and the only available lower bound using two extremum principles developed by Hill (*17*) and by Hill and Power (*18*) and later, from a different point of view, by Johnson (*19, 20*). [The velocity extremum principle was presented by Pawlowski (*15*) and by Bird (*21*).] The agreement between the calculated results and available experimental data was not entirely satisfactory.

In creeping flow past a sphere, $\sigma \to 0$ as distance from the solid surface increases. This suggests that the Ellis model, which correctly predicts a nonzero and finite viscosity in the limit as $\sigma \to 0$, might be a more satisfactory description of fluid behavior in this geometry than the power model. The purpose of this work is to calculate upper and lower bounds to the drag coefficient of a sphere in an Ellis model fluid and to compare the results with available experimental data and previous power model calculations. The upper and lower bounds are obtained by means of an original adaptation to the Ellis model fluid of the extremum principles of Hill (*17*) and of Hill and Power (*18*).

PROBLEM

The physical situation considered is a sphere falling very slowly at its terminal velocity through an unbounded fluid. A spherical coordinate system is fixed at the center of the sphere (θ measured from the + z axis and φ as measured from the + x axis in the x-y plane). The boundary conditions are that the velocity of the fluid is zero at the surface of the sphere

$$r = R : \mathbf{v} = 0 \tag{9}$$

and the fluid at infinity moves in the + z direction with a speed V_∞:

$$r \to \infty : v_r \to V_\infty \cos\theta, \quad v_\theta \to -V_\infty \sin\theta, \quad v_\phi \to 0 \tag{10}$$

Since the sphere falls at its terminal velocity, in terms of the coordinate system introduced, the motion of the fluid is independent of time.

We assume that the external force per unit mass $\mathbf{f}$ may be expressed in terms of a potential

$$\mathbf{f} = -\nabla\varphi \tag{11}$$

and we neglect all inertial effects with respect to viscous effects. The equation of motion becomes

$$\text{div}\,(\mathbf{T} - \rho\varphi\,\mathbf{I}) = 0 \tag{12}$$

We make a number of assumptions about the behavior of the fluid. We assume that it is incompressible, so that the equation of continuity reduces to

$$\text{div}\,\mathbf{v} = 0 \tag{13}$$

For the moment, we assume that the extra stress tensor $\mathbf{T}_E$ may be represented in terms of a scalar valued convex function $E = E(\gamma)$:

$$T_{Eij} = \frac{\partial E}{\partial D^{ij}} \tag{14}$$

By a convex function, we mean that

$$E(\gamma^*) - E(\gamma) \geqq \frac{\partial E}{\partial D^{ij}} [D^{*ij} - D^{ij}] \tag{15}$$

The field $\mathbf{D}^*$ differs somewhat from $\mathbf{D}$; in what follows below, we will identify $\mathbf{D}^*$ as an approximation for $\mathbf{D}$; the derivative $(\partial E)/(\partial D^{ij})$ is evaluated for $\mathbf{D}$. Similarly, we assume that we may represent the rate-of-deformation tensor in terms of a scalar valued convex function $E_c = E_c(\sigma)$:

$$D_{ij} = \frac{\partial E_c}{\partial T_E{}^{ij}} \tag{16}$$

Again, by the requirement that E_c be a convex function, we mean that

$$E_c(\sigma^*) - E_c(\sigma) \geqq \frac{\partial E_c}{\partial T_E{}^{ij}} [T_E{}^{*ij} - T_E{}^{ij}] \tag{17}$$

We will identify $\mathbf{T}_E{}^*$ as an aproximation for $\mathbf{T}_E$; the derivative $(\partial E_c)/(\partial T_E{}^{ij})$ is evaluated for $\mathbf{T}_E$. Hill and Power (*18*) [see also (*22*)] give the necessary and sufficient conditions that E and E_c be convex functions.

For a generalized Newtonian fluid of the form Equation (1), we have

$$E = \int_0^{\gamma^2} \eta(\gamma^2)\, d\gamma^2 \tag{18}$$

In order to represent Equation (6), we require

$$E_c = \int_0^{\sigma^2} \frac{1}{4}\,\Phi(\sigma^2)\, d\sigma^2 \tag{19}$$

EXTREMUM PRINCIPLES

The extremum principles used here have been developed previously by Hill (*17*) and by Hill and Power (*18*). Some of the details missing in their compact presentations have been given elsewhere (*22*).

Let us consider a simply or multiply connected domain V, the bounding surface of which is S. Let S_v be that portion of S upon which velocity is specified. Integrals of Equations (15) and (17) over V imply that (*22*)

$$\int_V E(\gamma^*)\, dV - \int_{S-S_v} (\mathbf{v}^* - \mathbf{v}) \cdot (\mathbf{T} - \rho\varphi\,\mathbf{I}) \cdot \mathbf{n}\, dS \geqq \int_V E(\gamma)\, dV \tag{20}$$

and that†

$$\int_V E(\gamma)\, dV \geqq -\int_V E_c(\sigma^*)\, dV + \int_S \mathbf{v} \cdot (\mathbf{T}^* - \rho\varphi\,\mathbf{I}) \cdot \mathbf{n}\, dS \tag{21}$$

We understand here that $\mathbf{v}^*$ is an approximate velocity distribution which satisfies the equation of continuity and the boundary conditions on velocity and which is continuous throughout the possibly multiply connected domain V (γ^* is defined in terms of $\mathbf{v}^*$). By $\mathbf{T}^*$ we mean an approximate stress distribution, which is continuous throughout V and which satisfies the equation of motion, Equation (12) (σ^* is defined in terms of $T_E{}^*$).

Equations (20) and (21) give upper and lower bounds on the volume integral of the extra stress potential E. Hill (*17*) gives an approximate method of relating E to the viscous dissipation per unit volume, but there is no way of estimating the errors involving in this approach. If E is homogeneous, as for the Newtonian and power model fluids, the viscous dissipation per unit volume is just a multiple of E. For the Ellis model, E is not homogeneous and can not be directly related to the viscous dissipation per unit volume.

For an Ellis model fluid, Equation (8), we have from Equation (19)

$$E_c = \frac{1}{4\eta_0} \left\{ 1 + \frac{2}{\alpha + 1} \left[\frac{\sigma}{\sqrt{2}\,\tau_{1/2}} \right]^{\alpha - 1} \right\} \sigma^2 \tag{22}$$

From Equations (6) and (8), we find that

$$tr(\mathbf{T}_E \cdot \mathbf{D}) = \frac{1}{2\eta_0} \left\{ 1 + \left[\frac{\sigma}{\sqrt{2}\,\tau_{1/2}} \right]^{\alpha - 1} \right\} \sigma^2 \tag{23}$$

It has been shown elsewhere (*17, 22*) that

$$E + E_c = tr\,(\mathbf{T}_E \cdot \mathbf{D}) \tag{24}$$

Equations (22) to (24) imply that

$$E = E(\sigma) = \frac{1}{4\eta_0} \left\{ 1 + \frac{2\alpha}{\alpha + 1} \left[\frac{\sigma}{\sqrt{2}\,\tau_{1/2}} \right]^{\alpha - 1} \right\} \sigma^2 \tag{25}$$

For the majority of fluids, $\alpha \geqq 1$ (*23*). If we restrict ourselves to $\alpha \geqq 1$, we see upon comparing Equations (23) and (25) that

---

† In (*1*), Equations (57), (58), and (59) should read, respectively:

$$\Psi_v = -v_i\, n_j\, (t^{ij} - \rho\,\varphi\, g^{ij})$$

$$\Psi_v = (p + \rho\,\varphi)\, v_r - (v_r\, \tau_{rr} + v_\theta\, \tau_{r\theta})$$

and

$$p + \rho\,\varphi = [-(A + F')\, x^4 \cos\theta + F'\, x^2 \cos\theta]\, m\, (2V/D)^n$$

$$tr\,(\mathbf{T}_E \cdot \mathbf{D}) \leq 2E \tag{26}$$

and

$$tr\,(\mathbf{T}_E \cdot \mathbf{D}) \geq \frac{\alpha+1}{\alpha} E \tag{27}$$

Equations (20), (21), (26), and (27) consequently allow us to calculate upper and lower bounds to the viscous dissipation of energy in the region V.

For the steady state, creeping flow past a sphere of an infinite body of incompressible fluid, the integral momentum balance (24), and the integral energy balance (24) may be used to obtain

$$V_\infty F_z = \int_V tr\,(\mathbf{T}_E \cdot \mathbf{D})\, dV \tag{28}$$

It is usually more convenient to speak in terms of the drag coefficient (or friction factor) f:

$$f = \frac{2F_z}{\rho V_\infty^2 \pi R^2} \tag{29}$$

Equations (20), (21), and (26) to (29) allow us to compute bounds on the drag coefficient for sphere in an Ellis model fluid.

UPPER BOUND

In order to employ Equation (20), we require a trial velocity distribution $\mathbf{v}^*$ which satisfies the equation of continuity and all boundary conditions in which velocity is specified. If we assume symmetry with respect to the z-axis and take $v_\phi = 0$, we may satisfy the equation of continuity by writing the two remaining velocity components in terms of a stream function:

$$v_r = -\frac{1}{r^2 \sin\theta}\frac{\partial \Psi}{\partial \theta}, \quad v_\theta = \frac{1}{r \sin\theta}\frac{\partial \Psi}{\partial r} \tag{30}$$

We use here a previously suggested one-parameter trial stream function (1):

$$\Psi^* = -\frac{1}{2} V_\infty r^2 \sin^2\theta \left[1 - \left(\frac{R}{r}\right)^a\right]^2 \tag{31}$$

In terms of this trial stream function, we find that

$$\bar{\gamma}^{*2} = 6a^2 x^{2(a+1)} \{[1 - x^a]^2 \cos^2\theta + \frac{1}{12}[a - 1 - (2a-1)x^a]^2 \sin^2\theta\} \tag{32}$$

For convenience, we define

$$\bar{\gamma} \equiv \frac{R\gamma}{V_\infty}, \quad x \equiv \frac{R}{r} \tag{33}$$

Through Equations (6) and (8) we may define $\bar{\sigma}^{**}$ in terms of $\bar{\gamma}^*$ by means of

$$\bar{\gamma}^{*2} = \frac{1}{4}\{1 + [N_1 \bar{\sigma}^{**}]^{\alpha-1}\}^2 \bar{\sigma}^{**2} \tag{34}$$

where

$$\bar{\sigma} \equiv \frac{R\sigma}{\eta_0 V_\infty}, \quad N_1 \equiv \frac{\eta_0 V_\infty}{\sqrt{2}\, R\tau_{1/2}} \tag{35}$$

With reference to Equation (20), velocity is specified on the entire bounding surface of the system in this problem, $S = S_v$. Consequently, Equation (25) allows Equation (20) to be written as

$$\frac{4}{R V_\infty^2 \eta_0}\int_V E(\gamma)\, dV \leq \frac{1}{R^3}\int_V \left\{1 + \frac{2\alpha}{\alpha+1}[N_1 \sigma^{**}]^{\alpha-1}\right\} \sigma^{**2}\, dV \tag{36}$$

Equations (26) to (29) and (36) may finally be arranged to yield

$$f N_2 \leq 4 \int_0^\pi \int_0^1 \left\{1 + \frac{2\alpha}{\alpha+1}[N_1 \bar{\sigma}^{**}]^{\alpha-1}\right\} \bar{\sigma}^{**2} x^{-4} \sin\theta\, dx\, d\theta \tag{37}$$

where we define

$$N_2 \equiv \frac{2R V_\infty \rho}{\eta_0} \tag{38}$$

The two integrals in Equation (37) were evaluated by using Simpson's rule in two dimensions. At each point and for each value of a, $\bar{\sigma}^{**}$ was calculated from Equations (32) and (34) by a Newton-Raphson iteration. The optimum value of a, corresponding to a minimum upper bound in inequality (37), was found by a Fibonacci search (25, p. 24).

LOWER BOUND

Any trial stress distribution $\mathbf{T}^*$ which satisfies the equation of motion, Equation (12), may be used to obtain a lower bound for $f N_2$ through Equations (21) and (27) to (29). We employ here a previously suggested one-parameter distribution (1):

$$T^*_{Er\theta} = -B\left(\frac{\eta_0 V_\infty}{R}\right) x^4 \sin\theta \tag{39}$$

$$T^*_{E\theta\theta} = T^*_{E\phi\phi} = -\frac{1}{2} T^*_{Err} = -B\left(\frac{\eta_0 V_\infty}{R}\right)(x^2 - x^4)\cos\theta \tag{40}$$

and

$$p^* + \rho\varphi = p_0 - B\left(\frac{\eta_0 V_\infty}{R}\right) x^2 \cos\theta \tag{41}$$

Here B is the parameter which must be determined. From Equations (7), (39), and (40), we find

$$\bar{\sigma}^{*2} = 2B^2 x^4 [x^4 \sin^2\theta + 3(1 - x^2)^2 \cos^2\theta] \tag{42}$$

Equations (39) to (41) allow us to evaluate the surface integral in inequality (21) as

$$\int_S \mathbf{v} \cdot (\mathbf{T}^* - \rho\varphi\,\mathbf{I}) \cdot \mathbf{n}\, dS = 4\pi \eta_0 R V_\infty^2 B \tag{43}$$

Equations (22) and (43) permit inequality (21) to be rewritten as

$$\frac{4}{R V_\infty^2 \eta_0}\int_V E(\gamma)\, dV \geq 16\pi B - \frac{1}{R^3}\int_V \left\{1 + \frac{2}{\alpha+1}[N_1 \bar{\sigma}^*]^{\alpha-1}\right\} \bar{\sigma}^{*2}\, dV \tag{44}$$

From Equation (42), the first integral on the right of inequality (44) may be evaluated as

$$\frac{1}{R^3}\int_V \bar{\sigma}^{*2}\, dV = 2\pi \int_0^\pi \int_0^1 \bar{\sigma}^{*2} x^{-4} \sin\theta\, dx\, d\theta = \frac{16}{3}\pi B^2 \tag{45}$$

From Equations (27) to (29), (44), and (45), we find that

$$f N_2 \geqq \frac{16 B[\alpha+1]}{\alpha} - \frac{16}{3}\frac{[\alpha+1]}{\alpha} B^2$$

$$- \frac{4B^{\alpha+1}}{\alpha} \int_0^{\pi} \int_0^{1} N_1{}^{\alpha-1} \left[\frac{\bar{\sigma}^*}{B} \right]^{\alpha+1} x^{-4} \sin\theta \, dx \, d\theta \qquad (46)$$

The integral in Equation (46) was evaluated by applying Simpson's rule in two dimensions. The computational error is estimated to be 1%; in several cases, the number of panels was doubled and redoubled with less than 1% change in result. The parameter B in Equations (39) to (41) was determined by requiring that the lower bound in inequality (46) be a maximum.

COMPARISON WITH EXPERIMENT

Figure 1 shows representative curves for $f N_2$ as a function of α and N_1. Remember that as $N_1 \to 0$, we approach Newtonian behavior; as $N_1 \to \infty$, we have the behavior corresponding to a power model fluid, Equation (5).

There are two sets of data available with which to compare the calculated bounds. Slattery and Bird (*12, 26*) measured the drag coefficient for spheres moving through six aqueous solutions of carboxymethyl cellulose (CMC), the behavior of which appeared to be representable by the Ellis model. Following a previous suggestion (*12*), we estimate that the inertial terms in the equation of motion may be neglected when

$$N_2 \left(\frac{\rho V_\infty{}^2}{\tau_{1/2}} \right)^{\alpha-1} < 0.1 \qquad (47)$$

The average of the upper and lower bounds to the drag coefficient for the Ellis model predicted the results of seventy-one experiments (142 data points) which satisfied inequality (47) with an average error of 29%.* For the same cases, Wasserman and Slattery's (*1*) average of the upper and lower bounds to the drag coefficient were in error on the average by only 18%.

Turian (*11, 27*) measured the drag coefficient for spheres in aqueous solutions of hydroxyethyl cellulose (HEC) and polyethylene oxide (PEO), the behaviors of all of which appeared to be representable by the Ellis model. His experiments were carried out in cylinders of various diameters, providing a means of determining wall effects on the drag coefficient. The velocity of the sphere in an infinite body of fluid was found by plotting the experimental velocity vs. the reciprocal of cylinder diameter and by extrapolating to infinite diameter. Only data which extrapolated well were used. The average of the upper and lower bounds to the drag coefficient for the Ellis model predicted the results of twenty-four experiments which satisfied inequality (47) with an average error of 16%.* For the same cases, Wasserman and Slattery's (*1*) average of the upper and lower bounds to the drag coefficient were in error by 58%.

The Ellis model should represent experimental data at least as well as the power model, since the former includes the latter as a limiting case. However, the results described above indicate that the calculations of Wasserman and Slattery, which were based upon the power model, on the average do a better job of representing the experimental data of Slattery and Bird than do the computations presented here for the Ellis model. For both sets of calculations, the computed values of the drag coefficient were consistently lower than the experimental values. One possible explanation for this is that in employing Equations (20), (21), and (26) to (29) we obtain bounds upon bounds. From Equations (26) and (27), we see that this becomes more serious as α increases beyond unity. Since α is considerably larger for Turian's data than it is for the data of Slattery and Bird, and since the computations presented here for the Ellis model were much more successful in predicting Turian's data than the computations of Wasserman and Slattery based upon the power model, it appears that there must be some other explanation.

There are some reasons to doubt the accuracy of Slattery's data. Wall effects are neglected; Turian (*11*) found the wall correction to be important. Slattery (*26*) states that the CMC solutions for the two experiments (capillary viscometer and flow past a sphere) were prepared separately; the behavior of the two mixes may not have been identical. A close examination of the data reveals that the apparent viscosity of the solutions seems to have been decreasing with time; for example, the measured velocity of the sphere increased with run number in most cases, even though the ratio of sphere diameter to cylinder diameter increased.

The drag coefficients from Turian's data were predicted much more accurately by the present computations based

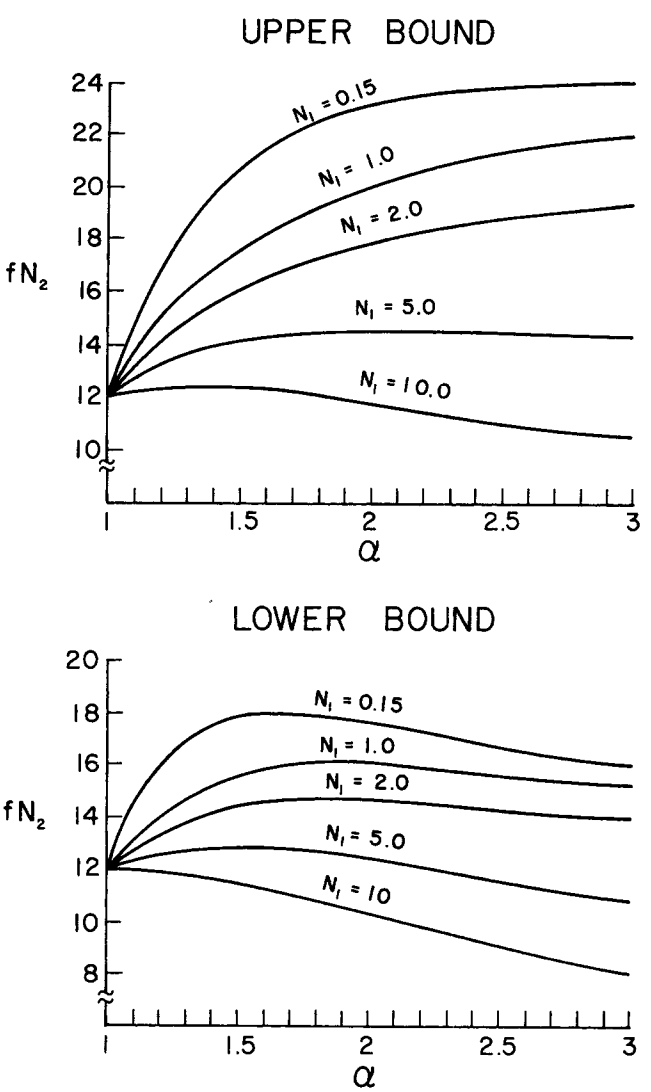

Fig. 1. Upper and lower bounds on $f N_2$ as functions of α for various values of N_1.

* A more detailed comparison of the present results and of the results of Wasserman and Slattery (*1*) with the experimental data of Slattery and Bird (*12, 26*) and of Turian (*11, 27*) has been deposited as document 00744 with the ASIS National Auxiliary Publications Service, c/o CMC Information Sciences, Inc., 22 W. 34 St., New York 10001 and may be obtained for $1.00 for microfiche and $3.00 for photocopies.

upon the Ellis model than by the calculations of Wasserman and Slattery from the power model. This is not surprising, since the plots of apparent viscosity vs. rate-of-deformation (*27*) indicate that the behaviors of the solutions were not represented well by the power model.

APPLICATIONS

One may be given a particular sphere and a particular fluid describable by the Ellis model and wish to determine the terminal velocity V_∞ of the sphere in the fluid. Such a calculation must be done by trial and error, with Figure 1 used in the following manner.

Choose a value of V_∞. Calculate the corresponding value of N_1 and use this value to determine from Figure 1 upper and lower bounds on fN_2. For a sphere of density $\rho_{(s)}$ falling at a constant velocity through a fluid of density $\rho_{(f)}$, the z component of the force which the fluid exerts on the sphere is

$$F_z = \frac{4}{3}\left[\rho_{(s)} - \rho_{(f)}\right] g \pi R^3 \tag{48}$$

From Equations (29) and (38), we find that

$$V_\infty = \frac{16}{3}\frac{\left[\rho_{(s)} - \rho_{(f)}\right] g R^2}{\eta_0}\frac{1}{f N_2} \tag{49}$$

By using the average of the upper and lower bounds of $f N_2$ found in Figure 1, calculate V_∞ from Equation (49). If the velocity which was assumed in calculating N_1 initially is the same as that determined from Equation (49), the bounds found for $f N_2$ are valid. If the velocities are different, the procedure must be repeated for another assumed value of V_∞.

Some readers may be tempted to take measured values of the drag coefficient and of the terminal velocity for a fluid of unknown character and attempt to deduce the corresponding Ellis model parameters. We do not recommend this for the following reasons.

1. There are many simple models which make up the class of generalized Newtonian fluids, Equation (*1*). It is much easier to discriminate among various models when looking at data from a viscometric flow rather than at data from a nonviscometric flow, since there is a generalized analysis available for the viscometric flows (*28, 29*).
2. Since we have found here only bounds on the drag coefficient, the analysis is not suitable for the deduction of accurate values for the Ellis model parameters.
3. Aspects of material behavior, which are not evident from observing pressure drop as a function of volume rate of flow through a tube, may be important for some materials in a (nonviscometric) flow such as movement past a sphere (*29*, p.7).

CONCLUSIONS

1. A method of adapting Hill's extremum principles to the Ellis model was developed.
2. A new method for calculating upper and lower bounds to the drag coefficient for a sphere moving slowly through an Ellis model fluid was developed.
3. Available experimental data from Slattery and Bird (*12, 26*) and from Turian (*11, 27*) were compared with the results of these calculations. Agreement was poor with Slattery's data and good with Turian's data. Some reasons to suspect Slattery's data have been pointed out.

NOTATION

a = undetermined parameter in Equation (31)
B = undetermined parameter in Equations (39) to (41)
$\mathbf{D}$ = rate of deformation tensor
$\mathbf{D}^*$ = approximate rate of deformation tensor defined in terms of $\mathbf{v}^*$
D_{ij}, D^{ij} = covariant and contravariant components of the rate of deformation tensor respectively
E = extra stress potential, Equation (14)
E_c = rate-of-deformation potential, Equation (16)
f = drag coefficient, Equation (29)
$\mathbf{f}$ = external force per unit mass
F_z = z component of force which the fluid exerts on the sphere
$\mathbf{I}$ = identity tensor
m, n = parameters in power model, Equation (5)
$\mathbf{n}$ = outwardly directed unit vector normal to the closed surface S
N_1, N_2 = defined by Equations (35) and (38), respectively
p = pressure
p_0 = undetermined reference pressure
r = spherical coordinate
R = radius of sphere
S = closed bounding surface of region V
S_v = portion of S on which velocity is specified
$\mathbf{T}$ = stress tensor
$\mathbf{T}^*$ = approximate stress distribution which is continuous throughout the possibly multiply connected domain V and which satisfies Equation (12)
$\mathbf{T}_E$ = extra stress tensor, Equation (1)
T_{Eij} = covariant components of the extra stress tensor
$T_{Err}, T_{E\theta\theta}, T_{E\phi\phi}, T_{Er\theta}$ = physical components of the extra stress tensor in spherical coordinates
$\mathbf{v}$ = velocity vector
$\mathbf{v}^*$ = approximate velocity distribution which satisfies Equation (13) and the boundary conditions on velocity and which is continuous throughout the possibly multiply connected domain V
v_r, v_θ, v_ϕ = physical components of velocity vector in spherical coordinates
V = domain occupied by fluid, may be multiply connected
V_z = speed in the positive z direction of fluid at infinity with respect to the center of the sphere
x = defined by Equation (33)

Greek Letters

$\alpha, \eta_0, \tau_{1/2}$ = parameters in Ellis model, Equation (8)
γ = defined by Equation (3)
γ^* = defined in terms of $\mathbf{D}^*$ by Equation (3)
$\bar{\gamma}$ = defined by Equation (33)
η = viscosity function, Equation (1)
θ = spherical coordinate measured from the positive z axis
ρ = density
σ = defined by Equation (7)
σ^* = defined in terms of $\mathbf{T}_E{}^*$ by Equation (7)
$\bar{\sigma}$ = defined by Equation (35)
$\bar{\sigma}^{**}$ = define by Equation (34)
φ = external force potential, Equation (11). Also used as third spherical coordinate as in Equation (10)
Φ = fluidity function, Equation (6)
ψ = axisymmetric stream function for spherical coordinate, Equation (30)
ψ^* = trial stream function corresponding to $\mathbf{v}^*$

LITERATURE CITED

1. Wasserman, M. L., and J. C. Slattery, *AIChE J.*, **10**, 383 (1964).
2. Slattery, J. C., *ibid.*, **11**, 831 (1965).

3. Reiner, Markus, *Am. J. Math.*, **67**, 350 (1945).
4. Rivlin, R. S., *Nature*, **160**, 611 (1947).
5. ———, *Proc. Roy. Soc. (London) Ser. A*, **193**, 260 (1948).
6. Serrin, James, "Handbuch der Physik," vol. 8/1, p. 231, S. Flugge, ed. Springer-Verlag, Berlin, Germany (1959).
7. Reiner, Markus, "Deformation, Strain, and Flow," p. 246, Interscience, New York (1960).
8. Sadowski, T. J., *Trans. Soc. of Rheol.*, **9**, No. 2, 251 (1965).
9. Ashare, Edward, R. B. Bird, and J. A. Lescarboura, *AIChE J.*, **11**, 910 (1965).
10. Sutterby, J. L., Ph.D. thesis, Univ. Wisc., Madison (1964).
11. Turian, R. M., *AIChE J.*, **13**, 999 (1967).
12. Slattery, J. C., and R. B. Bird, *Chem. Eng. Sci.*, **16**, 231 (1961).
13. Tomita, Yukio, *Bull. Japan. Soc. Mech. Engrs.*, **2**, 469 (1959).
14. Wallick, G. C., J. G. Savins, and D. R. Arterburn, *Phys. Fluids*, **5**, 367 (1962).
15. Pawlowski, J., *Kolloid Z.*, **138**, 6 (1954).
16. Slattery, J. C., *AIChE J.*, **8**, 663 (1962).
17. Hill, R., *J. Mech. Phys. Solids*, **5**, 66 (1956).
18. Hill, R., and G. Power, *Quart. J. Mech. Appl. Math.*, **9**, 313 (1956).
19. Johnson, M. W., Jr., *Phys. Fluids*, **3**, 871 (1960).
20. ———, *Trans. Soc. Rheol.*, **5**, 9 (1961).
21. Bird, R. B., *Phys. Fluids*, **3**, 539 (1960).
22. Ehrlich, Robert, and John C. Slattery, *Ind. Eng. Chem. Fundamentals*, **7**, 239 (1968).
23. Bird, R. B., *Can. J. Chem. Eng.*, **8**, 161 (1965).
24. ———, *Chem. Eng. Sci.*, **6**, 123 (1957).
25. Wilde, D. J., "Optimum Seeking Methods," Prentice-Hall, Englewood Cliffs, N. J. (1964).
26. Slattery, J. C., Ph.D. thesis, Univ. Wisc., Madison (1959).
27. Turian, R. M., Ph.D. thesis, Univ. Wisc., Madison (1963).
28. Rabinowitsch, B., *Z. physik. Chem.*, **A145**, 1 (1929).
29. Coleman, B. D., H. Markovitz, and W. Noll, "Viscometric Flows of Non-Newtonian Fluids," Springer-Verlag, New York (1966).

Manuscript received December 26, 1967; revision received August 19, 1968; paper accepted August 21, 1968.

A New Simulation Method for Equilibrium Stage Processes

JOHN F. TOMICH

Esso Production Research Company, Houston, Texas

This paper presents a new, general method for mathematical simulation of equilibrium stage operations. The procedure solves component material balance equations with a tridiagonal matrix algorithm. Heat balances and summation equations are handled with Broyden's method. The unique feature of this procedure is that, in a mathematical sense, all equations are solved simultaneously. Therefore, the method can be used for all types of equilibrium stage processes. Additionally, the use of Broyden iteration insures solutions which are both stable and more rapid than current techniques. An exact solution for a twenty tray column with twenty components takes approximately 30 sec. on an IBM 360/65 computer. Successful simulations have been made for both absorption and distillation type of operations which have included complex columns with multiple feeds and side product streams. Design applications of the method cover a variety of equilibrium stage processes in the chemical and petroleum industries.

Countercurrent flow, mass transfer columns are primary unit operations used for separation in the chemical and petroleum industries. Methods for solving the equations simulating specific types of these column processes are known (*1* to 7). There is, however, need for a more efficient, general calculation method which will predict component distributions and temperature profiles in all types of towers, even complex units with multiple feeds and widely varying temperatures and vapor flow rates. Procedures in current use as well as those reported in the literature work well for either absorption or distillation type of problems, but in general cannot be applied to both. Although many of the column processes used are of these two types, many do not conveniently fit into either category. Rich oil demethanizers in natural gas processing plants, for example, usually have absorption characteristics over a certain part of the column and distillation characteristics over another.

This paper describes a new method which provides stable, rapid solutions to the mass and energy balance equations associated with all kinds of tower processes. The procedure is highly numerical, but with digital computers it can be applied to many tower design problems. The method is generally applicable to all countercurrent flow